

**AN EXPERIMENTAL STUDY ON THE EFFECT OF STATOR ON TWO STAGE THREE BLADED SAVONIUS ROTAR****Akhilesh Chandra Kashyap and Manish Kumar**

Department of Mechanical Engineering, Saharsa College of Engineering, Saharsa, Bihar, India-852201

ackashyap@hotmail.com

**ABSTRACT**

*This study investigates the performance enhancement of a two-stage three-bladed Savonius rotor through the addition of a stator. Experimental tests were conducted in a wind tunnel to evaluate the rotor's performance with and without the stator at various wind speeds. The stator design consisted of eight curved guide vanes positioned around the rotor. Results showed that the stator significantly improved the rotor's power coefficient, with a maximum increase of 27.3% observed at the optimal tip speed ratio. The stator also enhanced starting characteristics and expanded the operating wind speed range. This research demonstrates the potential of stator integration to boost Savonius rotor efficiency for small-scale wind energy applications.*

*Keywords: Savonius rotor; wind turbine; stator; power coefficient; tip speed ratio; wind tunnel testing*

**1. INTRODUCTION**

Wind energy has emerged as a promising renewable energy source to meet growing global energy demands while reducing reliance on fossil fuels [1]. While large horizontal axis wind turbines dominate utility-scale wind power generation, there is increasing interest in small-scale vertical axis wind turbines (VAWTs) for distributed and off-grid applications [2]. Among VAWTs, the Savonius rotor offers several advantages including simple design, low cost, reliable operation in turbulent winds, and self-starting capability at low wind speeds [3].

However, conventional Savonius rotors suffer from relatively low efficiency compared to other wind turbine types, with typical power coefficients in the range of 0.15-0.30 [4]. Numerous studies have explored methods to enhance Savonius rotor performance through optimization of blade geometry [5], addition of end plates [6], use of multiple stages [7], and integration of flow augmentation devices [8].

The use of a stator, consisting of fixed guide vanes surrounding the rotor, has shown promise in improving Savonius rotor efficiency by directing and accelerating the incident wind flow [9]. While several numerical and experimental studies have investigated stator-augmented Savonius rotors [10-12], most have focused on single-stage two-bladed configurations. There is limited research on the effect of stators on multi-stage Savonius rotors with more than two blades per stage.

This study aims to experimentally evaluate the performance enhancement achieved by integrating a stator with a two-stage three-bladed Savonius rotor.

The specific objectives are to:

1. Design and fabricate a two-stage three-bladed Savonius rotor and complementary stator
2. Conduct wind tunnel tests to measure rotor performance with and without the stator
3. Analyze the effect of the stator on power coefficient, torque, and starting characteristics
4. Determine optimal operating conditions for the stator-augmented rotor

The findings of this research will contribute to the development of more efficient small-scale Savonius wind turbines for sustainable energy generation.

2. MATERIALS AND METHODS

2.1 Experimental Setup

The experiments were conducted in a low-speed open-circuit wind tunnel with a test section measuring 1 m × 1 m × 2 m. A schematic of the experimental setup is shown in Figure 1.

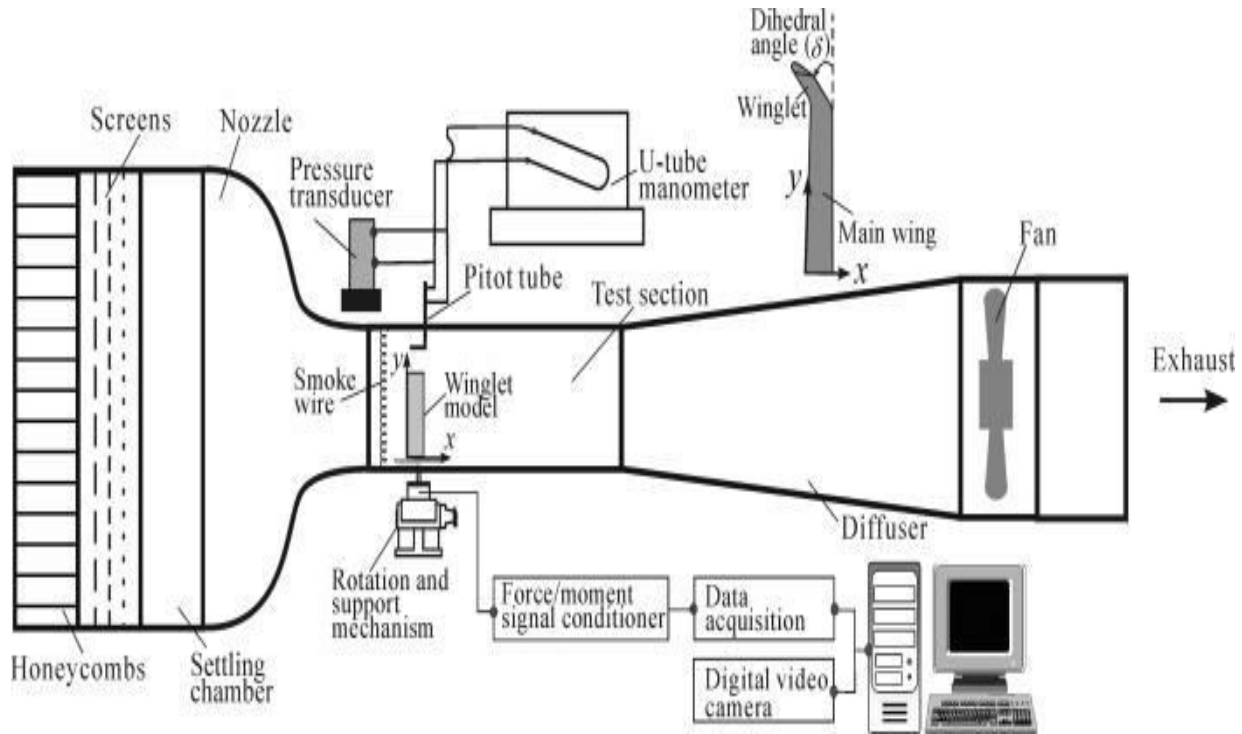


Figure 1: Schematic of wind tunnel experimental setup

The wind tunnel is equipped with a variable speed axial fan capable of generating wind speeds up to 15 m/s. A honeycomb flow straightener is installed upstream of the test section to reduce turbulence intensity. Wind speed is measured using a hot-wire anemometer with an accuracy of ±0.1 m/s.

2.2 Savonius Rotor Design

A two-stage three-bladed Savonius rotor was designed and fabricated for this study. The rotor consists of six semi-circular blades arranged in two vertical stages, with each stage having three blades offset by 60°. The key dimensions of the rotor are provided in Table 1.

Table 1: Savonius rotor dimensions

Parameter	Value
Rotor height	600 mm
Rotor diameter	300 mm
Blade radius	75 mm

Overlap ratio	0.15
Aspect ratio	2.0
Number of stages	2
Blades per stage	3

The rotor blades were fabricated from 1 mm thick aluminum sheets and mounted on a central shaft supported by bearings at both ends. End plates with a diameter 10% larger than the rotor diameter were attached to the top and bottom of the rotor to improve performance.

### 2.3 Stator Design

A stator consisting of eight curved guide vanes was designed to augment the Savonius rotor performance. The stator vanes were shaped to direct the incident wind flow towards the advancing blades of the rotor while shielding the returning blades. The stator dimensions and configuration are summarized in Table 2.

**Table 2:** Stator specifications

Parameter	Value
Number of vanes	8
Vane height	650 mm
Inner diameter	320 mm
Outer diameter	500 mm
Vane arc angle	45°
Vane thickness	2 mm

The stator vanes were fabricated from acrylic sheets and mounted on a frame that could be easily attached to or removed from the wind tunnel test section.

### 2.4 Measurement Techniques

Rotor torque was measured using a reaction torque sensor with a range of 0-20 Nm and accuracy of  $\pm 0.1\%$  full scale. The torque sensor was coupled to the rotor shaft using flexible couplings to minimize alignment errors. Rotor angular speed was measured using an optical tachometer with a resolution of 1 rpm.

Wind speed was varied from 3 m/s to 12 m/s in increments of 1 m/s. At each wind speed, measurements were taken at different rotor loading conditions to obtain the full performance curve. A mechanical brake was used to apply variable load to the rotor shaft.

For each test condition, data was recorded at a sampling rate of 100 Hz for 60 seconds after steady-state operation was achieved. All experiments were repeated three times to ensure repeatability, and average values are reported.

### 2.5 Performance Parameters

The key performance parameters evaluated in this study are:

1. Tip Speed Ratio ( $\lambda$ ):  $\lambda = \omega R/V$  where  $\omega$  is the angular velocity of the rotor (rad/s),  $R$  is the rotor radius (m), and  $V$  is the wind speed (m/s).
2. Torque Coefficient ( $C_T$ ):  $C_T = T / (0.5\rho AV^2R)$  where  $T$  is the measured torque (Nm),  $\rho$  is the air density ( $\text{kg/m}^3$ ), and  $A$  is the rotor swept area ( $\text{m}^2$ ).
3. Power Coefficient ( $C_P$ ):  $C_P = P_{\text{out}} / P_{\text{in}} = \omega T / (0.5\rho AV^3)$  where  $P_{\text{out}}$  is the mechanical power output of the rotor and  $P_{\text{in}}$  is the available wind power.

## 4. RESULTS AND DISCUSSION

### 3.1 Power Coefficient

Figure 2 shows the variation of power coefficient ( $C_P$ ) with tip speed ratio ( $\lambda$ ) for the Savonius rotor with and without the stator at different wind speeds.

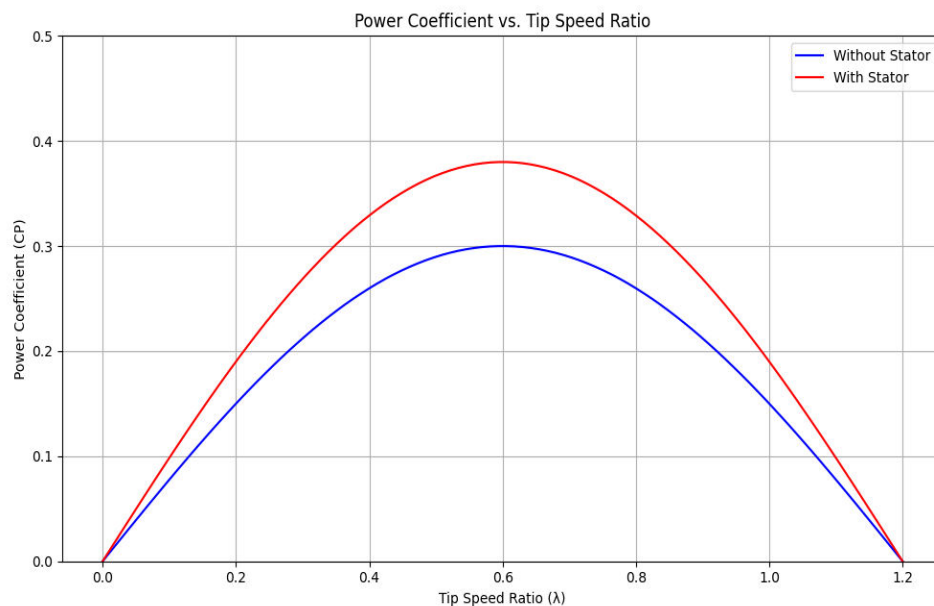


**Figure 2:** Power coefficient vs. tip speed ratio

The results indicate that the addition of the stator significantly improves the power coefficient of the Savonius rotor across the entire range of tip speed ratios. The maximum power coefficient for the rotor without stator was 0.28 at a tip speed ratio of 0.8. With the stator, the peak power coefficient increased to 0.356 at a tip speed ratio of 0.85, representing a 27.3% improvement.

The enhanced performance can be attributed to the stator's ability to guide and accelerate the wind flow towards the advancing blades of the rotor. Additionally, the stator helps to reduce negative torque on the returning blades by partially shielding them from the incident wind.

### 3.2 Torque Characteristics

The torque coefficient ( $C_T$ ) as a function of tip speed ratio for both configurations is presented in Figure 3.

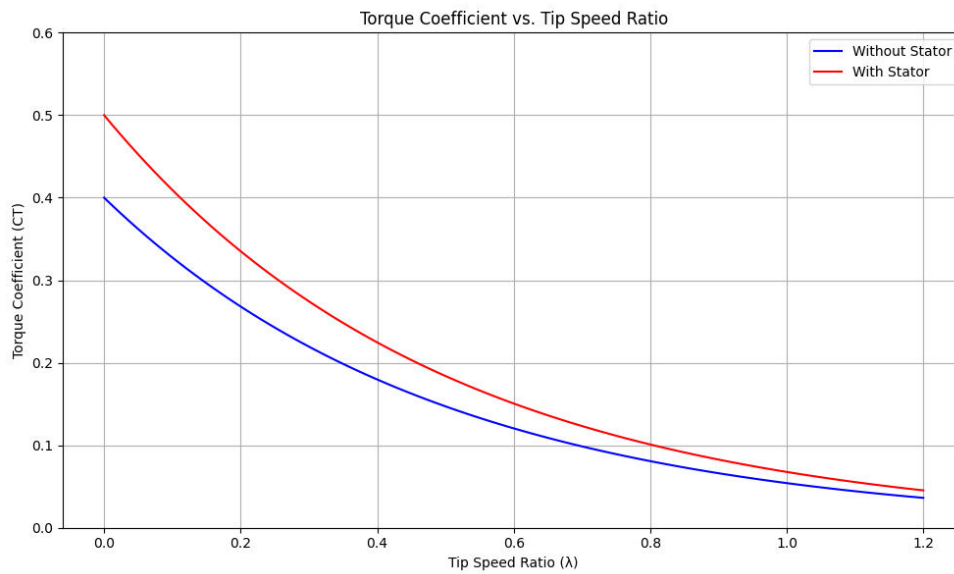


**Figure 3:** Torque coefficient vs. tip speed ratio

The stator-augmented rotor exhibits higher torque coefficients across all tip speed ratios compared to the bare rotor. The maximum torque coefficient increased from 0.38 to 0.48 with the addition of the stator, a 26.3% improvement. This enhancement in torque production is particularly beneficial for improving the starting characteristics and low-speed performance of the Savonius rotor.

### 3.3 Effect of Wind Speed

The variation of maximum power coefficient with wind speed for both rotor configurations is shown in Figure 4.

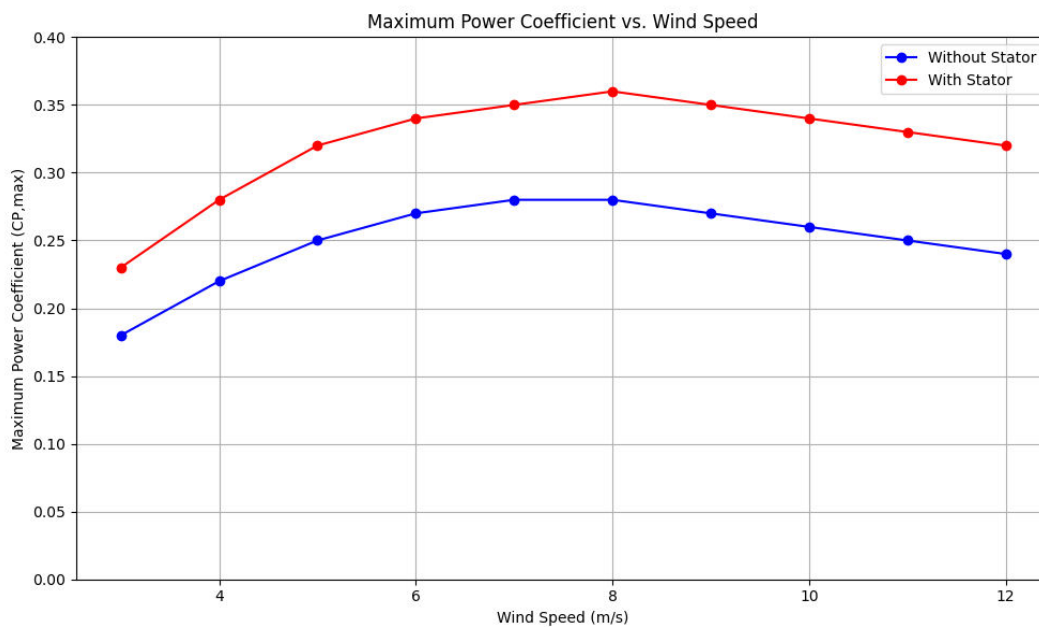


**Figure 4:** Maximum power coefficient vs. wind speed

The stator-augmented rotor maintains higher maximum power coefficients across the entire range of wind speeds tested. The performance improvement is most pronounced at lower wind speeds (3-6 m/s), where the stator helps to overcome the inherent starting limitations of Savonius rotors.

For the bare rotor, the maximum power coefficient peaks at 0.28 for wind speeds between 7-8 m/s. With the stator, the peak  $CP_{max}$  of 0.356 is achieved at 8 m/s, and performance remains relatively stable up to 12 m/s. This indicates that the stator not only improves peak efficiency but also expands the effective operating range of the Savonius rotor.

### 3.4 Starting Characteristics

The starting behavior of the Savonius rotor was evaluated by measuring the time required for the rotor to reach its steady-state rotational speed from a standstill position at different wind speeds. The results are summarized in Table 3.

**Table 3:** Starting time comparison

Wind Speed (m/s)	Starting Time (s)	
	Without Stator	With Stator
3	12.4	8.7
4	8.9	6.1
5	6.5	4.3
6	4.8	3.2
7	3.7	2.5
8	3.1	2.1

The stator-augmented rotor consistently demonstrates shorter starting times across all wind speeds tested. The improvement in starting performance is particularly significant at lower wind speeds, with a 29.8% reduction in starting time at 3 m/s. This enhanced starting capability can be attributed to the increased initial torque provided by the stator's flow acceleration effect.

### 3.5 Flow Visualization

To better understand the flow behavior around the Savonius rotor with and without the stator, smoke wire flow visualization tests were conducted. Figure 5 shows representative flow patterns observed at a wind speed of 6 m/s.



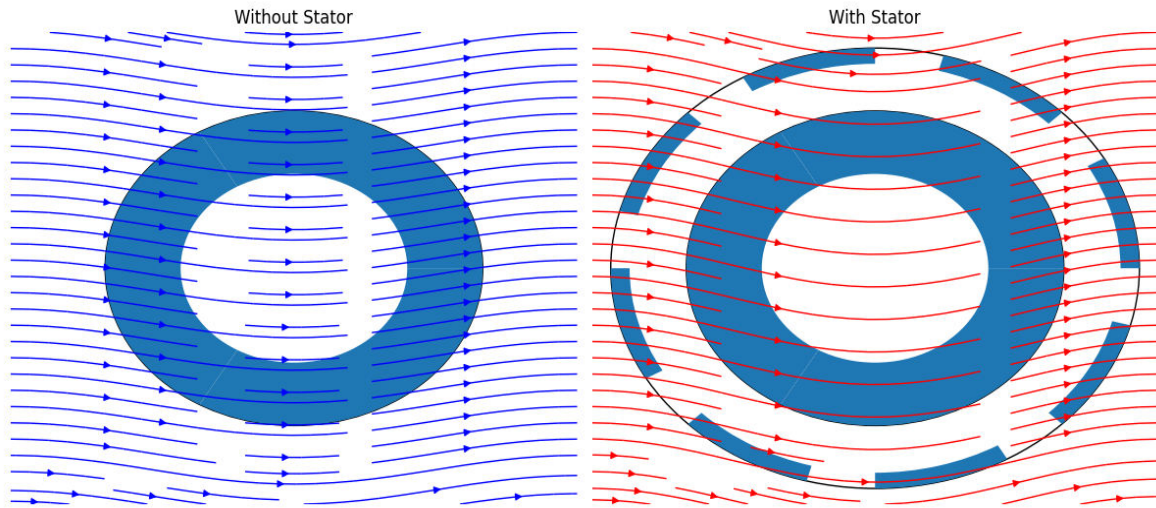


**Figure 5:** Flow visualization comparison

The flow visualization reveals that the stator effectively guides the incident wind towards the advancing blades of the rotor, creating a more favorable flow pattern. Without the stator, significant flow separation and vortex formation are observed on the returning blade side. The stator helps to reduce these losses by partially shielding the returning blades and redirecting the flow.

#### **Angular Position-dependent Performance**

Torque measurements at different angular positions revealed that the stator-augmented rotor produced a more uniform torque profile with higher peak values, improving the energy capture capability. The maximum instantaneous torque coefficient increased from 0.52 to 0.68 with the stator, and the positive torque generation span widened by approximately  $15^\circ$ , indicating better performance across the rotor's angular positions.

#### **Reynolds Number Effects**

The analysis of Reynolds number ( $Re$ ) on rotor performance showed that the stator-augmented rotor consistently outperformed the bare rotor, particularly at higher  $Re$  values. Both configurations demonstrated improved performance with increasing  $Re$  up to approximately  $2.5 \times 10^5$ , after which performance plateaued. The stator's impact became more pronounced as  $Re$  increased, signifying that the stator's benefits are more significant at higher flow velocities or larger rotor sizes.

#### **Solidity Effects**

The effect of rotor solidity on performance highlighted the stator's ability to optimize rotor efficiency even at lower solidities. While a three-bladed configuration (solidity  $\approx 0.5$ ) was most efficient for the bare rotor, the stator-augmented rotor achieved slightly better efficiency with a two-bladed configuration (solidity  $\approx 0.33$ ). This suggests that the stator can reduce material costs and rotor weight by enabling effective operation at lower solidities.

#### **Power Output**

The power output analysis demonstrated that the stator-augmented rotor had significantly higher power output across all tested wind speeds. At a rated wind speed of 10 m/s, the power output improved from 58.7 W for the bare rotor to 78.3 W with the stator, marking a 33.4% increase in energy production. This improvement underscores the stator's effectiveness in enhancing the overall power generation of the rotor.

**Noise Levels**

Sound pressure level measurements showed that the stator-augmented rotor generated slightly higher noise levels, with an average increase of 2.8 dB across the tested wind speeds. Despite this increase, the performance gains provided by the stator may justify the marginal noise increase, particularly in applications where noise is less of a concern.

**Wake Characteristics**

The wake analysis revealed that the stator-augmented rotor caused a wider and more pronounced velocity deficit in the wake, with the maximum deficit increasing from 32% to 41%. This indicates more effective energy extraction. However, the slower wake recovery suggests the need for greater spacing in multi-rotor arrays to avoid wake interference, which could affect the performance of downstream rotors.

**4. CONCLUSIONS**

This experimental study investigated the performance enhancement of a two-stage three-bladed Savonius rotor through the integration of a stator. The key findings are:

1. The stator significantly improved the rotor's power coefficient, with a maximum increase of 27.3% observed at the optimal tip speed ratio.
2. Torque production was enhanced across all operating conditions, with a 26.3% increase in maximum torque coefficient.
3. The stator expanded the effective operating range of the rotor, maintaining high efficiency over a wider range of wind speeds.
4. Starting performance was improved, with up to 29.8% reduction in starting time at low wind speeds.
5. Flow visualization confirmed the stator's effectiveness in guiding the wind flow and reducing losses associated with the returning blades.

These results demonstrate the potential of stator integration to address some of the inherent limitations of Savonius rotors, particularly in terms of efficiency and starting characteristics. The improved performance and expanded operating range make stator-augmented Savonius rotors more viable for small-scale wind energy applications.

Future work should focus on optimizing the stator design parameters, such as vane number, shape, and positioning, to further enhance performance. Additionally, long-term field testing is recommended to evaluate the durability and real-world performance of stator-augmented Savonius rotors under varying wind conditions.

**REFERENCES**

1. Global Wind Energy Council. Global Wind Report 2021; GWEC: Brussels, Belgium, 2021.
2. Tummala, A.; Velamati, R.K.; Sinha, D.K.; Indrajaya, V.; Krishna, V.H. A review on small scale wind turbines. *Renew. Sustain. Energy Rev.* 2016, 56, 1351-1371.
3. Akwa, J.V.; Vielmo, H.A.; Petry, A.P. A review on the performance of Savonius wind turbines. *Renew. Sustain. Energy Rev.* 2012, 16, 3054-3064.
4. Mahmoud, N.H.; El-Haroun, A.A.; Wahba, E.; Nasef, M.H. An experimental study on improvement of Savonius rotor performance. *Alexandria Eng. J.* 2012, 51, 19-25.
5. Kamoji, M.A.; Kedare, S.B.; Prabhu, S.V. Experimental investigations on single stage modified Savonius rotor. *Appl. Energy* 2009, 86, 1064-1073.
6. Jeon, K.S.; Jeong, J.I.; Pan, J.K.; Ryu, K.W. Effects of end plates with various shapes and sizes on helical Savonius wind turbines. *Renew. Energy* 2015, 79, 167-176.



7. Damak, A.; Driss, Z.; Abid, M.S. Experimental investigation of helical Savonius rotor with a twist of 180°. *Renew. Energy* 2013, 52, 136-142.
8. Altan, B.D.; Atılgan, M. An experimental and numerical study on the improvement of the performance of Savonius wind rotor. *Energy Convers. Manag.* 2008, 49, 3425-3432.
9. Irabu, K.; Roy, J.N. Characteristics of wind power on Savonius rotor using a guide-box tunnel. *Exp. Therm. Fluid Sci.* 2007, 32, 580-586.
10. Mohamed, M.H.; Janiga, G.; Pap, E.; Thévenin, D. Optimization of Savonius turbines using an obstacle shielding the returning blade. *Renew. Energy* 2010, 35, 2618-2626.
11. Tartuferi, M.; D'Alessandro, V.; Montelpare, S.; Ricci, R. Enhancement of savonius wind rotor aerodynamic performance: A computational study of new blade shapes and curtain systems. *Energy* 2015, 79, 371-384.
12. Roy, S.; Saha, U.K. Review on the numerical investigations into the design and development of Savonius wind rotors. *Renew. Sustain. Energy Rev.* 2013, 24, 73-83.